



OPEN

Physiologically-based pharmacokinetic modeling for optimal dosage prediction of olaparib when co-administered with CYP3A4 modulators and in patients with hepatic/renal impairment

Dongmei Gao¹, Guopeng Wang², Honghai Wu³ & Jiawei Ren⁴✉

This study aimed to develop a physiologically-based pharmacokinetic (PBPK) model to predict the maximum plasma concentration (C_{max}) and trough concentration (C_{trough}) at steady-state of olaparib (OLA) in Caucasian, Japanese and Chinese. Furthermore, the PBPK model was combined with mean and 95% confidence interval to predict optimal dosing regimens of OLA when co-administered with CYP3A4 modulators and administered to patients with hepatic/renal impairment. The dosing regimens were determined based on safety and efficacy PK threshold C_{max} (<12,500 ng/mL) and C_{trough} (772–2500 ng/mL). The population PBPK model for OLA was successfully developed and validated, demonstrating good consistency with clinically observed data. The ratios of predicted to observed values for C_{max} and C_{trough} fell within the range of 0.5 to 2.0. When OLA was co-administered with a strong or moderate CYP3A4 inhibitor, the recommended dosing regimens should be reduced to 100 mg BID and 150 mg BID, respectively. Additionally, the PBPK model also suggested that OLA could be not recommended with a strong or moderate CYP3A4 inducer. For patients with moderate hepatic and renal impairment, the dosing regimens of OLA were recommended to be reduced to 200 mg BID and 150 mg BID, respectively. In cases of severe hepatic and renal impairment, the PBPK model suggested a dosing regimen of 100 mg BID for OLA. Overall, this present PBPK model can determine the optimal dosing regimens for various clinical scenarios involving OLA.

Olaparib (OLA) is a first-in-class poly ADP-ribose polymerase (PARP) inhibitor and was approved in 2014 by FDA¹. It is clinically indicated for the treatment of patients with ovarian or breast cancer^{1,2}. In clinic, a 400 mg capsule formulation twice daily (BID) (16 × 50 mg large capsules) was first approved for treatment³. Afterwards, a tablet formulation of 300 mg BID (4 × 150 mg tablet) was developed to enhance patient compliance by reducing the number and size of units required to achieve a therapeutic dose³. The approved tablet dosage strengths for patients are 100 mg and 150 mg².

OLA is partially hepatically cleared and metabolized primarily by CYP3A4¹. Additionally, Approximately 44% of OLA is cleared by the kidney and excreted through urine⁴. The in vitro study showed that OLA was efficiently transported by human ABCG2 and ABCB1 (P-gp)⁵. Moreover, in the in vitro assessments, OLA showed the inhibition of multiple hepatic and renal uptake transporters, suggesting the strongest inhibition

¹Department of Medical Oncology, Bethune International Peace Hospital, Shijiazhuang 050082, China. ²Zhongcai Health (Beijing) Biological Technology Development Co., Ltd., Beijing 101500, China. ³Department of Clinical Pharmacy, Bethune International Peace Hospital, Shijiazhuang 050082, China. ⁴North China Electric Power University, No.2, Beinong Road, Huilongguan, Changping District, Beijing 102206, China. ✉email: rjw@ncepu.edu.cn

against transporter MATE1 with an IC_{50} of 5.5 μM ⁶. Furthermore, in a study, OLA significantly induced CYP3A4 enzyme expression⁷.

The in vitro study revealed that a concentration of 1 μM OLA (equivalent to 435 ng/mL) is required for effective inhibition of various cancer cell lines, including those with BRCA mutant, low BRCA expression, and no-BRCA expression^{4,8}. Notably, for cell lines with low BRCA and no-BRCA mutant expression, higher concentrations of OLA were necessary to achieve comparable clinical efficacy⁴. This is likely because, in cell lines expressing higher levels of BRCA mutations, the DNA damage repairment heavily relies on base excision repair, in which PARP plays a crucial role. In contrast, in cell lines exhibiting lower levels of BRCA mutations, DNA repair can still occur through the homologous recombination repair mechanism. As a result, higher concentrations of OLA are necessary to achieve desired efficacy. Additionally, in a BRCA2 breast cancer mouse model, tumor reduction was only observed at doses that sustained exposure above the IC_{50} for more than 13 h⁴. Furthermore, these findings from the in vitro study have been also further supported by clinical trials conducted in humans⁴. In the clinic, no statistically significant difference was observed in the overall response rate (ORR) and progression-free survival (PFS) between the 400 mg BID and 200 mg BID doses^{4,9}. As a result, the 200 mg BID was identified as the lowest efficacy dose. The mean trough concentration (C_{trough}) of OLA at 200 mg is 960 ng/mL¹⁰, 500 ng/mL¹¹, and 855 ng/mL¹² in the three clinical research studies, respectively. As a result, the pharmacokinetic (PK) threshold for optimum clinical efficacy was identified as a mean C_{trough} of ≥ 772 ng/mL. In a retrospective study¹³, there was a strong correlation between OLA exposure and early adverse events in patients with BRCA1/2 mutations. As a result, a C_{trough} of ≤ 2500 ng/mL was identified as a clinical safety PK threshold. The analyses of C_{max} -anemia relationship in patients have suggested that the frequency of anemia in patients can reach approximately 55% when the C_{max} is above 12,500 ng/mL⁴. Overall, for optimal clinical efficacy and a safe profile, C_{trough} should be limited within 772–2500 ng/mL, and C_{max} is below 12,500 ng/mL.

The human AUC, C_{trough} and C_{max} of OLA can be influenced by multiple factors, including concomitant use with CYP3A4 perpetrators (drug–drug interactions, DDIs), and use in patients with insufficient hepatic/renal function. Previous studies have shown that co-administration of OLA with itraconazole (a strong CYP3A4 inhibitor) increased its AUC by 42%³, while co-administration with rifampicin (a strong CYP3A4 inducer) decreased its AUC by 72%³. Additionally, the clinical study also showed that patients with renal impairment had a 1.75-fold increase in AUC and a 1.39-fold increase in C_{max} of OLA compared to patients with normal renal function¹⁴.

When administering OLA to patients in various clinical scenarios, such as concurrent use with other CYP3A4 modulators or in patients with hepatic/renal impairment, it may be necessary to make dosing adjustments. When determining the optimum dosing regimens for OLA, it is important to consider the C_{trough} and C_{max} threshold as a key factor. To aid in this process, a PBPK model was developed in patients to (1) predict the C_{trough} and C_{max} of OLA in Caucasian, Japanese and Chinese patients, respectively; (2) predict C_{trough} and C_{max} alterations of OLA when combined use with CYP3A4 modulators, and use in Caucasian patients with insufficient hepatic/renal function; and (3) recommend an optimal dosing regimen in multiple clinical situations according to the C_{trough} and C_{max} threshold.

Materials and methods

Virtual population demographic characteristics

The demographic characteristics utilized in each simulation were derived from the corresponding clinical study. PK-Sim incorporates information such as age range, body weight, height, and proportion of female individuals from the virtual population data. In cases where the clinical studies do not provide specific demographic characteristics, similar studies are referenced to obtain relevant data for the simulations. In situations where certain data are unavailable, PK-Sim employs default values or values from similar studies as substitutes. To ensure an adequate sample size, if the number of subjects in the clinical studies is less than 10, 10 virtual subjects are created for the simulations. The demographic characteristics of the virtual population used in the simulations are summarized in Table 1.

| Races | Clinical studies | Number of subjects | Age range | Proportion of female (%) | Population |
|------------------------------|-------------------------------|--------------------|-----------|--------------------------|------------|
| Caucasian | Fong et al. ¹⁰ | 17 | 19–82 | 67 | Patients |
| | Dean et al. ¹¹ | 10 | 22–71 | 100 | |
| | | | 33–60 | 75 | |
| | Mateo et al. ²² | 17 | 35–75 | 100 | |
| Plummer et al. ²³ | 27 | 29–71 | 87 | | |
| Japanese | Yamamoto et al. ¹² | 10 | 54–67 | 33 | Patients |
| | | | 39–69 | 66 | |
| | Yonemori et al. ²⁰ | 10 | 37–55 | 57 | |
| Japanese | Yuan et al. ²¹ | 20 | 44–64 | 100 | Patients |
| | | | 50–65 | 65 | |

Table 1. Demographic data of race in virtual population.

Software

The PBPK model was constructed using the PK-Sim® (Version 10.0, Bayer Technology Services, Leverkusen, Germany); PK profiles of OLA from published papers were digitized using Digit (Version 1.0.4, Simulations Plus, USA), and the figures were drawn using Origin 2019 (version 9.6.5.169, OriginLab, USA).

PBPK model development

The three parameters (K_p , scale, partition coefficients, and cellular permeabilities) are crucial in predicting drug distribution in body. In PK-Sim, five different methods are employed to determine tissue distribution: Rodgers and Rowland, PK-Sim standard, Schmitt, Poulin, Theil, and Berezhkovskiy. Cellular permeability, on the other hand, is calculated using two methods: PK-Sim standard and Charge dependent Schmitt. To enhance the alignment of predicted OLA concentration–time profiles with observed PK profiles, the distribution calculation for OLA in the PBPK model was optimized using the parameter identification module in PK-Sim. The method selected for tissue distribution calculation was Rodgers and Rowland, while the PK-Sim standard method was chosen for cellular permeability calculation. Furthermore, to further improve the agreement between predicted and observed PK of OLA, the K_p scale was optimized to 1.5. OLA has mean plasma protein binding of 89% observed at multiple concentrations⁴, f_{up} was hence set at 0.11. There were no reports indicating that kidney transporters or tubules are involved in the influx or efflux of OLA. Therefore, the fraction of GFR was set to 1.0. The efflux transport of OLA was described by intrinsic transport velocity (CL_{int}). The P-gp $CL_{int,u}$ was estimated as 0.63 $\mu\text{L}/\text{min}/\text{million cells}^{-1}$ from the P_{eff} (effective permeability) data in transfected MDCKII/h ABCB1⁵. Similarly, ABCG2 $CL_{int,u}$ was calculated to be 0.27 $\mu\text{L}/\text{min}/\text{million cells}^{-1}$ in transfected MDCKII/h ABCG2 using the same method⁵. The renal clearance (CL_R) was calculated using the glomerular filtration rate (GFR) $\times f_{up}$ method in PK-Sim®. The PBPK model of OLA contains one metabolizing enzyme (CYP3A4) and two efflux transporters (ABCB1 and ABCG2). Because the PK-Sim® expression database did not include the reference concentrations of the two transporters, the reference concentration for ABCB1 and ABCG2 were calculated to be 0.68 and 0.13 $\mu\text{M}/\text{L}$ liver tissue, respectively, using the formula (transporter abundance \times expressed organ weight)/liver volume¹⁵.

OLA is clinically available in two formulations, namely capsule and tablet, and there are two notable differences observed between the in vitro dissolution and in vivo PK. Compared to tablets, OLA capsules exhibit a slower dissolution rate and lower bioavailability¹⁶. The Weibull time parameter is a modeling parameter that can be utilized to characterize the speed of drug dissolution. Therefore, Weibull times for capsule and tablet were set at 60 and 30 min, respectively. Additionally, because the clinical bioavailability study of two dosage forms revealed that the AUC of 300 mg BID tablet was similar to that of 400 mg BID capsule¹⁶, the CYP3A4 $CL_{int,u}$ values, which are associated with AUC, were assigned as 0.058 and 0.044 $\mu\text{L}/\text{min}/\text{pmol}$ for capsule and tablet, respectively. Similarly, HLM $CL_{int,u}$ (human liver microsome) values for capsule and tablet were assigned as 0.22 and 0.17 $\mu\text{L}/\text{min}/\text{mg protein}$, respectively¹⁶.

When developing PBPK population models, the most commonly considered known inter-ethnic physiological differences include variations in height and weight distribution, metabolizing enzyme abundances, and liver volume¹⁷. In this PBPK model, the default liver volume was used at 2.38, 216 and 1.91 L for Caucasian, Japanese and Chinese, respectively. On the basis of literature data¹⁸, the CYP3A4 abundance was set at 137, 112 and 120 pmol/mg protein for Caucasian, Japanese, and Chinese, respectively. Table 2 summarizes the final parameters of the model, which were derived from various sources^{1,4,5,7,16,18,19}. Figure 1 illustrates the generic workflow of the PBPK model.

PBPK model validation

The clinically observed PK data of OLA in Caucasian^{10,11}, Japanese^{12,20}, and Chinese²¹ patients were used to validate the predictive performance of the PBPK model by comparing the coincidence of predicted and observed PK profiles. Next, this model was also verified by comparing the ratios between the observed and predicted C_{max} and C_{trough} ^{10–12,20–23}. Generally, the common acceptable criterion is between 0.5 and 2.0. It was assumed that steady state would be reached if OLA was taken BID for 14 consecutive days.

Sensitivity analysis

The sensitivity analysis were performed to evaluate the impact of selected model parameters on the C_{max} and C_{trough} , respectively. Patients were given standard dose regimens of 300 mg BID for 14 consecutive days. For the sensitivity analysis, both optimized and modeling parameters that were likely to have a significant influence on the C_{max} and C_{trough} were selected. The selected parameters were (1) $\log P$, (2) f_{up} , (3) R_{bp} , (4) CYP3A4 $CL_{int,u}$ (5) P-gp $CL_{int,u}$ and ABCG2 $CL_{int,u}$, (6) K_i CYP3A4, (7) EC_{50} and E_{max} for CYP3A4 (8) expression (CYP3A4, P-gp, ABCG2), and (9) liver volume.

To evaluate the impact of the selected parameters on C_{max} and C_{trough} , each parameter was altered by $\pm 20\%$ ²⁴. The sensitivity coefficient (SC) is estimated as follows²⁴:

$$SC = \Delta Y/Y \div \Delta P/P \quad (1)$$

where ΔY represents the alteration of predicted C_{max} or C_{trough} ; Y represents the start value of predicted C_{max} or C_{trough} ; ΔP is the change of modeling parameters; P represents start value of parameters. If a certain SC absolute value is greater than 1.0, it indicates that a 20% change in the evaluated parameter will result in a 20% change in predicted C_{max} or C_{trough} . It signifies the model parameter has a significant impact on C_{max} or C_{trough} .

| Property (Units) | Values used in the model | Literature values and source | Descriptions |
|-----------------------------------------------------------------|-----------------------------------------------------------|-----------------------------------------------------------------------------------------|------------------------------------------------------------------|
| MW(g·mol ⁻¹) | 434.46 | Chemspider | Molecular weight |
| pKa (Acid) | 12.07 | 12.07 ¹⁹ | Acid dissociation constant |
| LogP | 1.49 | 1.49 ¹⁹ | Lipophilicity |
| Solubility (mg·mL ⁻¹) | 0.12 | 0.12 (Water) ¹⁹ | Solubility in water |
| P _{eff} (× 10 ⁻⁴ cm s ⁻¹) | 36.2 | 36.2 ⁴ | Human effective permeability |
| f _{up} | 0.11 | 0.18 ⁴ | Fraction of free drug in plasma |
| Rbp | 0.80 | 0.80 ¹ | Blood-to-plasma concentration ratio |
| CYP3A4 CL _{int,u} (μL/min/pmol) | 0.058 ^a , 0.044 ^b | 0.058 ^{4,16} | Intrinsic clearance for CYP3A4 and HLM |
| Additional HLM CL _{int,u} (μL/min/mg) | 0.22 ^a , 0.17 ^b | 0.22 ^{4,16} | |
| CYP3A4 abundance (pmol/mg protein) | 137 ^c , 112 ^d , 120 ^e | 137 ^a , 112 ^b , 120 ^{c,18} | Content of CYP3A4 protein in liver microsomes |
| Liver volume (L) | 2.38 ^c , 2.16 ^d , 1.91 ^e | default | Liver volume |
| P-gp CL _{int,u} (μL/min/million cells ⁻¹) | 0.63 (Estimated) | P _{app} (10 ⁻⁶ cm/s): 37.3 for P-gp and 27.4 for ABCG2 ⁵ | Intrinsic transport velocity for P-gp and ABCG2 |
| ABCG2 CL _{int,u} (μL/min/million cells ⁻¹) | 0.27 (Estimated) | | |
| CL _R (L/h) | GFR*f _{up} | Default | Renal clearance |
| GFR fraction | 1.0 | Default | Fraction of filtered drug in the urine |
| K _p scale | 1.5 | Optimized | Organ-to-plasma partition coefficient |
| Partition coefficients | Rodgers and Rowland | Optimized | Calculation method from cell to plasma coefficients |
| Cellular permeabilities | PK-Sim Standard | | Permeability calculation method across cell |
| Weibull time (min) | 60 ^a , 30 ^b | Optimized | Dissolution time of 50% drug |
| Weibull shape | 0.62 | Default | Shape parameter of Weibull function |
| Concentration (μM/L liver tissue) | CYP3A4 | 4.32 | Reference concentration for metabolizing enzyme and transporters |
| | ABCB1 | 0.68 | |
| | ABCG2 | 0.13 | |
| K _i CYP3A4 (μM) | 72.2 | 14.3 ⁷ | Reversible inhibition constant at CYP3A4 |
| K _{inact} CYP3A4 (min ⁻¹) | 0.068 | 0.072 ⁷ | The maximum rate of inactivation against CYP3A4 |
| EC ₅₀ CYP3A4 (μM) | 18.0 | 18.0 ⁷ | Half-maximal induction |
| E _{max} CYP3A4 | 57.6 | 57.6 ⁷ | Maximum in vitro induction effect |

Table 2. Summary of parameters used in the PBPK model. ^a Capsule, ^b Tablet, ^c Caucasian, ^d Japanese, ^e Chinese.

DDI simulations

The final modeling parameters of five modulators are given in supplementary Table S1. Table 3 summarizes the inhibition and induction parameters of five modulators^{7,25–27}. In validating the DDI simulations, based on the literature's data³, the dosage regimens of OLA were designed as 300 mg OD in patients for consecutive 14 days. The dosage regimens of itraconazole and rifampicin were set at 200 mg OD and 600 mg OD, respectively, for 10 days (from day 5 to day 14). The virtual demographic data for DDI simulations involving itraconazole and rifampicin were sourced from a published paper³. The DDI simulations were first validated by comparing the differences between the predicted and observed PK profiles when concurrently administered with itraconazole and rifampicin³. Subsequently, the PBPK model for OLA was integrated with the PBPK models of CYP3A4 inhibitors (ketoconazole, itraconazole, and fluconazole) and inducers (rifampicin and efavirenz), respectively, to predict the C_{max} and C_{trough} of OLA when co-administered with five CYP3A4 modulators.

Simulations in patients with hepatic/renal impairment

The physiological parameters and characteristics for patients with inadequate hepatic or renal function were obtained from published papers and are presented in supplementary Table S2,S3. The virtual population demographic characteristics are presented in supplementary Table S4,S5. In hepatic impairment simulations, the default liver volume is 2.38 L in normal population in the PK-Sim[®]. Based on literature ratio data²⁸, liver volumes were calculated to be 2.12, 1.69, and 1.45 L in patients with wild, moderate and severe hepatic impairment, respectively. According to the paper²⁹, the fractional CYP3A4 CL_{int,u} value in patients with severe impairment was 0.4 of that in normal humans. The CYP3A4 abundance ratio of moderate to severe impairment was used to calculate the fractional CYP3A4 CL_{int,u} value (0.72) in moderate impairment patients. The actually determined albumin levels in normal, wild, and moderately impaired patients were obtained from the paper³⁰. Albumin levels in severe impairment patients calculated using the ratio of severe to normal (0.6)²⁸. The Plasma Protein Scale Factor (PPSF) in PK-Sim was utilized to account for variations in plasma albumin protein levels and unbound OLA fraction. PPSF is estimated³¹:

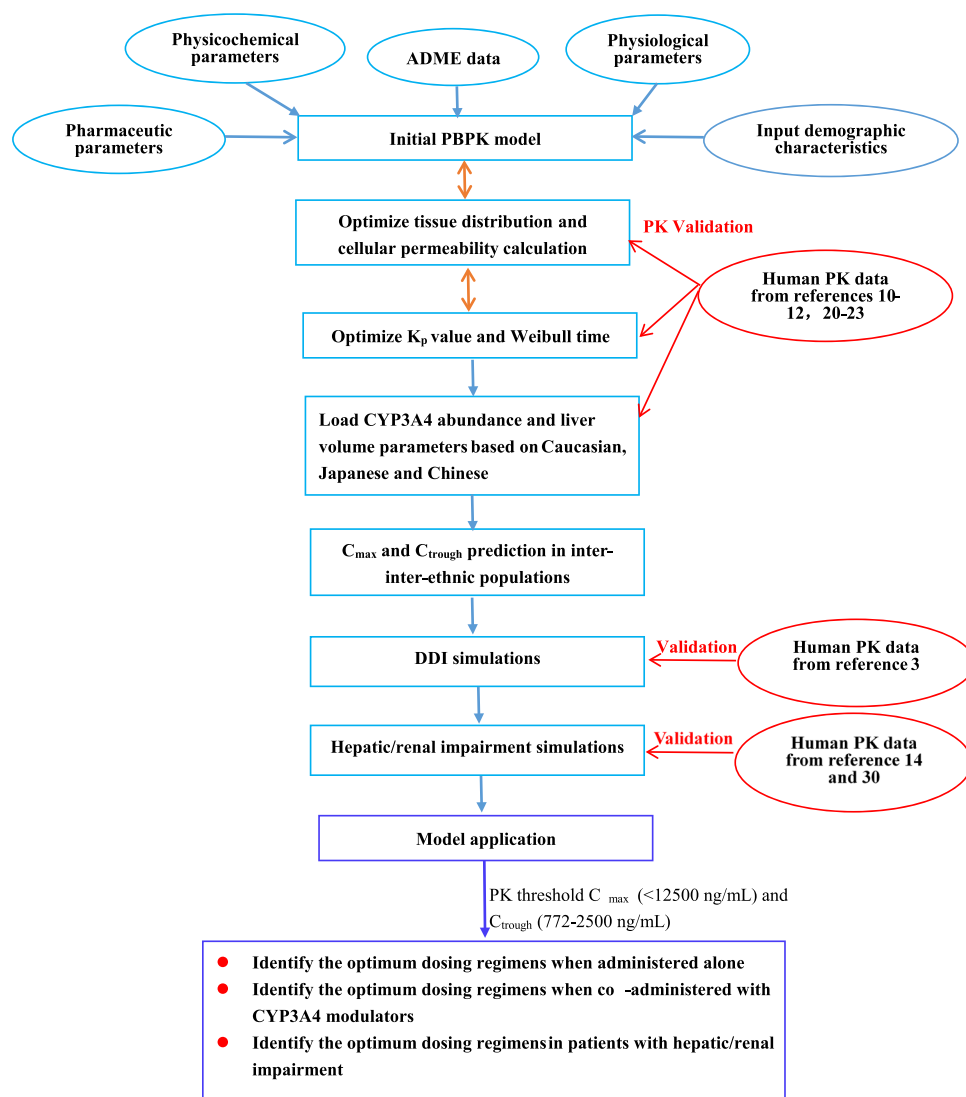


Figure 1. The generic workflow of the PBPK model for OLA. The population PBPK model was constructed using modeling parameters that encompassed the absorption, metabolism, and distribution processes associated with the CYP3A4 metabolizing enzyme, as well as the P-gp and ABCG2 transporters. The model was validated using multiple PK profiles in Caucasian, Japanese, and Chinese patients^{10-12,20,21}. The model was then further verified using ratios between predicted and observed C_{max} and C_{trough}^{10-12,20-23}. DDIs and hepatic/renal impairment simulations were also validated using PK profiles in patients when co-administered with itraconazole and rifampicin³, using PK profiles in patients with hepatic/renal impairment^{14,30}. Finally, the PBPK model was used to determine the optimal dosing regimens in various clinical scenarios.

| Modulators | K _i (μM) | EC _{max} | EC ₅₀ (μM) |
|-------------------------------------|---------------------|-------------------|-----------------------|
| Itraconazole ²⁵ | 0.0013 (CYP3A4) | – | – |
| Hydroxy-itraconazole ^{25a} | 0.0023 (CYP3A4) | – | – |
| Ketoconazole ²⁶ | 0.015 (CYP3A4) | – | – |
| Fluconazole ²⁷ | 16.6 (CYP3A4) | – | – |
| Rifampicin ⁷ | – | 121 (CYP3A4) | 0.92 |
| Efavirenz ^b | – | 5.2 (CYP3A4) | 0.07 |

Table 3. The inhibition and induction parameters of modulators. ^ametabolite of itraconazole; ^bbuilt in the PK-Sim®.

$$PPSF = \frac{1}{f_{up} + (1 - f_{up}) \times \text{Albumin}_f} \quad (2)$$

where Albumin_f is the fractional value of plasma albumin in patients with hepatic/renal impairment with respect to normal individuals.

In renal impairment simulations, renal blood flow (RBF) is estimated by the following formula³²:

$$\ln(\text{RBF}) = -3 \times 10^{-5} \times \text{GFR}^2 + 0.0170 \times \text{GFR} + 4.09 \quad (3)$$

Kidney volume (KV) is estimated by the following formula³²:

$$\ln(\text{KV}) = -6.3 \times 10^{-5} \times \text{GFR}^2 + 0.0149 \times \text{GFR} + 4.13 \quad (4)$$

Based on the literature's data^{14,30}, The dosage regimens of OLA were set at 300 mg OD for patients with wild, moderate, and severe hepatic/renal impairment in the simulations. The simulations in patients with hepatic/renal impairment were validated by comparing the predicted and observed PK data^{14,30}. Subsequently, the PBPK model was employed to forecast the C_{\max} and C_{trough} values in patients with mild, moderate, and severe hepatic or renal impairment, respectively following multiple doses of OLA given over a period of 14 consecutive days.

Human and animal rights

No human participants or cells were involved in this study, and the data were derived from publicly available sources.

Results

Validation of the PBPK model

Figure 2 shows the predicted and observed plasma concentration–time profiles in Caucasian (Fig. 2A–H), Japanese (Fig. 2I–L) and Chinese (Fig. 2M–N). The simulations showed that the developed population PBPK model may match the observed PK profiles^{10–12,21,22}. As seen in Table 4, all the ratios of predicted and observed geometric mean C_{\max} and C_{trough} were within 0.5–2.0, and most of predicted/observed ratios were in the range of 0.7–1.3. This suggests that this population PBPK model can predict accurately the C_{\max} and C_{trough} of OLA at steady state in different population ancestry. Moreover, the ratios of prediction to observation were found to be between 0.69 and 1.69 in the Caucasian population, 0.72–1.70 in the Japanese population, and 0.79–1.37 in the Chinese population. These results indicate that there are no significant differences in the ratios among the three inter-ethnic groups.

Sensitivity analysis

As shown in Fig. 3, the ten sensitive parameters to the OLA C_{\max} (Fig. 3A) and C_{trough} (Fig. 3B) are represented. The most sensitive parameter was Log P (SC: -0.61) for C_{\max} at steady-state. The sensitive parameters for C_{trough} were f_{up} (SC: -2.62), CYP3A4 expression (SC: -1.70), CYP3A4CL_{int,t} (SC: -1.65) and liver volume (SC: -1.32) at steady-state. Also of note was that four SC values for C_{trough} were more than 1.0. Overall, sensitivity analysis revealed the majority of modeling parameters had a slight impact on the C_{\max} and C_{trough} of OLA.

DDI simulations

The predicted and clinically observed PK profiles and data of five CYP3A4 inhibitors have been given in supplementary Figure S1 and Table S6. The predicted PK profiles of OLA with itraconazole and rifampin are shown in Fig. 4A,B. The 90% prediction interval almost covered the variability of the clinically observed PK data. The PK ratios predicted by the PBPK model are summarized in Table 5. The predicted C_{\max} , C_{trough} , and AUC_{312–336} ratios of OLA when dosed with itraconazole were 1.37-, 7.05- and 2.85-fold higher, respectively, compared to OLA alone. Conversely, Co-administration of OLA with rifampin resulted in a significantly predicted reduction in OLA C_{\max} , C_{trough} , and AUC_{312–336} ratios of 0.50, 0.13 and 0.17. The predicted C_{\max} , C_{trough} and AUC_{288–312} ratios of OLA by the PBPK model were very close to the clinically observed values (Table 5)³.

Simulations in patients with hepatic/renal impairment

Figure 4C–F and supplementary Table S7 show the predicted and observed PK profiles and data in patients with hepatic/renal impairment. All ratios between prediction and observation fell in the range of 0.5–2.0 (Table S7). Table 6 summarizes the predicted and observed ratios of C_{\max} , C_{24} and AUC_{0–96} in patients with mild, moderate and severe hepatic/renal impairment. The simulations showed that the predicted PK ratios were in agreement with the observed values^{14,30}. As seen in Table 6, the geometric mean C_{\max} and AUC_{0–96} were slightly increased for mild, moderate and severe hepatic/renal impairment patients within 2.0-fold. However, meaningfully increase occurred for C_{24} ranging from 1.1- to 6.3-fold in all hepatic/renal impairment patients. Overall, the PBPK model could reasonably predict the influence of hepatic/renal impairment on the PK change of OLA. This indicates the developed PBPK model can predict C_{\max} and C_{trough} in patients with liver/kidney impairment.

Dosage adjustment recommendation based on the PBPK model

As shown in Fig. 5, the optimal dosing regimens of OLA for each of the ethnic groups were studied based on the geometric mean and 95% confidence interval (95% CI) of the predicted C_{\max} and C_{trough} . The PBPK model supported the optimal dosing regimens of 300 and 400 mg BID in capsule formulation, and of 300 mg BID in tablet formulation (see Fig. 5). The conclusion is in good agreement with the clinical recommendations^{2,4}.

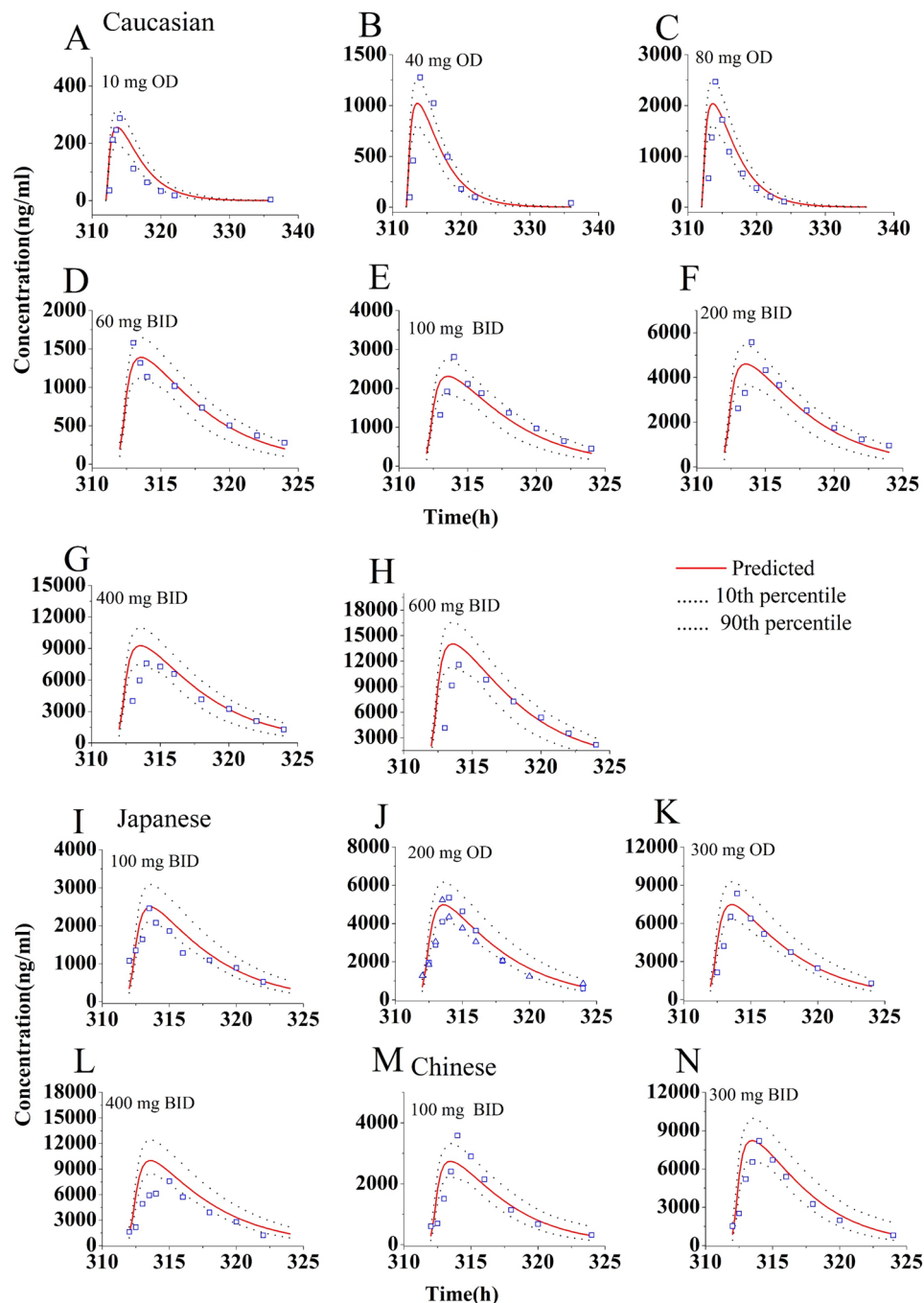


Figure 2. Simulations of the pharmacokinetics of OLA after administration of repeated doses. Blue squares and up-triangles are the clinically observed data.

Figure 6A,B shows the suitable dosing regimens for OLA under DDIs. Table 7 summarizes dosing adjustment recommendations under DDIs based on the PBPK model. As shown in Fig. 6A,B and Table 6, the PBPK model supported dose reduction when co-administered with CYP3A4 inhibitors. Dosage regimens were suggested to be adjusted to 50, 100 and 150 mg BID, respectively, when dosed with 200 mg OD itraconazole, 400 mg OD ketoconazole, and 200 mg OD fluconazole. Conversely, the PBPK model suggested to avoid concomitant use with CYP3A4 inducers (rifampicin and efavirenz). The simulations showed that dosing adjustment recommendations by the PBPK model were different from the based-AUC ratio recommendations.

Figure 6C–F depicts the OLA suitable dosing regimens for patients with hepatic/renal impairment. Based on the PBPK model, Table 7 summarizes dosing adjustment recommendations in patients with hepatic/renal impairment. As shown in Fig. 6C–F and Table 7, the PBPK model supported dose unchanged in patients with

| Clinical study | Ancestry | Dose (mg BID) /dosage form | No. of subjects | Age range/mean (year) | Proportion of female | C_{max} (ng/mL, range/CV % ^a) | | C_{trough} (ng/mL, range/CV %) | | Prediction/observation ratio | |
|-------------------------------|-----------|----------------------------|-----------------|-----------------------|----------------------|---------------------------------------------|----------------------|----------------------------------|------------------------|------------------------------|--------------------|
| | | | | | | Prediction | Observation | Prediction | Observation | C_{max} ratio | C_{trough} ratio |
| Fong et al. ¹⁰ | Caucasian | 200/Cap ^b | 17 | 19–82 | 0.67 | 4618 (3686–6854) | 5620 (2830–17,100) | 658 (276–999) | 960 (210–2950) | 0.82 | 0.69 |
| | | 400/Cap | 6 | | | 9283 (7418–13,806) | 7650 (5280–10,500) | 1340 (558–2029) | 1290 (660–3890) | 1.21 | 1.04 |
| | | 600/Cap | 5 | | | 14,034 (11,225–20,905) | 11,500 (6490–17,600) | 2072 (861–3126) | 2180 (390–5950) | 1.22 | 0.95 |
| Dean et al. ¹¹ | | 200/Cap | 4 | 22–71 | 1.0 | 4747 (3530–6015) | 4700 (35.6%) | 698 (134–2055) | 500 (191.2%) | 1.01 | 1.40 |
| | | 400/Cap | 4 | 33–60 | 0.75 | 9750 (7468–12,080) | 9100 (27.2%) | 1544 (357–3721) | 1600 (46.1%) | 1.07 | 0.97 |
| Mateo et al. ²² | | 400/ Cap | 10 | 50.9 | 0.91 | 9659 (7244–12,075) | 5710 (2380–10,900) | 1489 (319–3872) | 1860 (530–6670) | 1.69 | 0.80 |
| | | 400/ Cap | 17 | 52.5 | 1.0 | 9428 (7487–11,458) | 6360 (3880–13,300) | 1398 (362–2992) | 1040 (230–8490) | 1.48 | 1.34 |
| | | 200/Tab ^c | 13 | 59.1 | 1.0 | 6605 (5159–8302) | 6880 (4010–10,400) | 892 (148–2813) | 1000 (230–3100) | 0.96 | 0.89 |
| | | 300/Tab | 17 | 55.8 | 1.0 | 9944 (7762–1250) | 9370 (2280–14,700) | 1358 (225–4254) | 1840 (340–3830) | 1.06 | 0.74 |
| | | 400/Tab | 10 | 54.2 | 1.0 | 13,320 (10,387–16,747) | 12,000 (8450–16,900) | 1845 (308–5735) | 2010 (760–3610) | 1.11 | 0.92 |
| Plummer et al. ²³ | | 300/Tab | 27 | 29–71 | 0.87 | 10,062 (8091–12,379) | 9500 (4800–19,700) | 1444 (296–3697) | 2000 (600–11,400) | 1.06 | 0.72 |
| Yamamoto et al. ¹² | Japanese | 200/Cap | 3 | 54–67 | 0.33 | 4971 (4228–6177) | 4800 (31.6%) | 696 (460–1084) | 855 (NR ^d) | 1.04 | 0.81 |
| | | 400/Cap | 6 | 39–69 | 0.66 | 10,017 (8481–24,350) | 5900 (19.7) | 1413 (934–2202) | 1220 (NR) | 1.70 | 1.16 |
| Yonemori et al. ²⁰ | | 200/Tab | 3 | 37–55 | 0.57 | 6480 (4453–9037) | 7670 (46.9%) | 675 (376–1357) | 610 (157%) | 0.84 | 1.11 |
| | | 300/Tab | 6 | 44–64 | 1.0 | 9749 (6693–13,604) | 8430 (35.1%) | 1025 (567–2065) | 1290 (157.6%) | 1.16 | 0.79 |
| Yuan et al. ²¹ | Chinese | 300/Tab | 20 | 50–65 | 0.65 | 11,303 (9482–16,019) | 8270 (35%) | 1019 (459–2838) | 800 (118%) | 1.37 | 1.27 |

Table 4. Comparisons of the geometric mean C_{max} and C_{trough} between predicted and observed data in different population ancestry. ^aCV %, percentage coefficient of variation; ^bCap, capsule; ^cTab, Tablet; ^dNR, not reported.

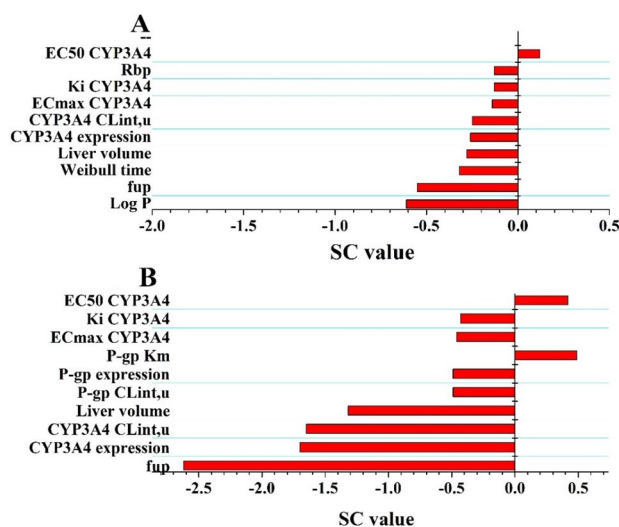


Figure 3. Sensitivity analysis of the PBPK model for C_{max} (A) and C_{trough} (B).

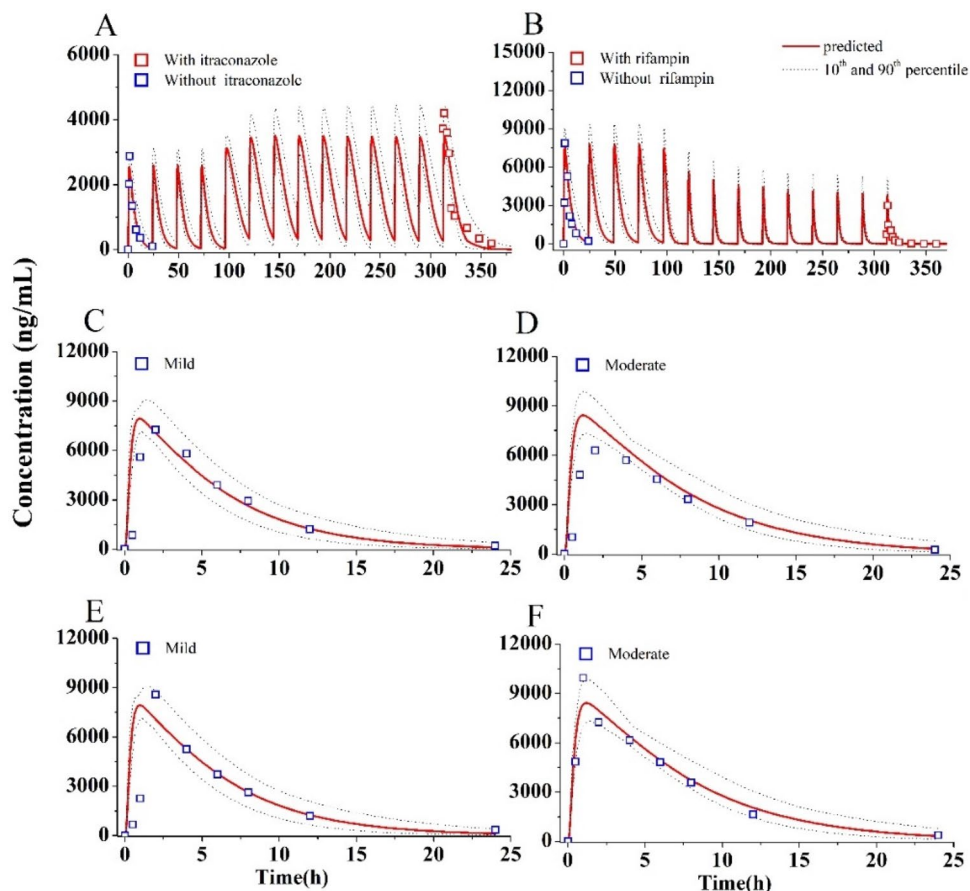


Figure 4. Simulations of pharmacokinetics of OLA (100 mg OD) with itraconazole (A), OLA (300 mg OD) with rifampin (B), in patients with mild (C) and moderate (D) hepatic impairment, in patients with mild (E) and moderate (F) renal impairment.

| Parameters | OLA only (100 mg OD) | OLA + Itraconazole (100 mg OD + 200 mg OD) | Predicted ^a ratio | Observed ratio |
|-------------------------------------------------|----------------------|--------------------------------------------|------------------------------|----------------|
| C_{max} (ng·mL ⁻¹) | 2560 | 3513 (2998–4463) | 1.37 | 1.41 |
| C_{trough} (ng·mL ⁻¹) | 39.1 | 275.6 (61.7–1450) | 7.05 | 6.56 |
| AUC _{312–336} (ng·h·mL ⁻¹) | 14,382 | 40,931(28,155–67,045) | 2.85 | 2.71 |
| Parameters | OLA only (300 mg OD) | OLA + Rifampin (300 mg OD + 600 mg OD) | Predicted ratio | Observed ratio |
| C_{max} (ng·mL ⁻¹) | 7818 | 3878 (2638–5222) | 0.50 | 0.82 |
| C_{trough} (ng·mL ⁻¹) | 115 | 25(15–324) | 0.13 | 0.05 |
| AUC _{312–336} (ng·h·mL ⁻¹) | 52,485 | 9012 (6268–13,979) | 0.17 | 0.12 |

Table 5. PK changes (geometric mean, range) of OLA under DDIs. ^aCalculated by ratio of concomitant to only use.

mild hepatic/renal impairment, and supported dose reduction in patients with moderate and severe hepatic/renal impairment.

The PBPK model suggested that dosing regimens should be reduced to 200 mg BID and 100 mg BID in patients with moderate and severe hepatic impairment, respectively. In addition, dosing regimens in patients with moderate and severe renal impairment should be reduced to 150 mg BID and 100 mg BID, respectively. However, the dosage recommendation by the PBPK model is different from the recommended dosing for patients with moderate and severe hepatic/renal impairment based on AUC ratio.

Discussion

In this work, the PK thresholds of OLA C_{max} (< 12,500 ng/mL) and C_{trough} (772–2500 ng/mL) at steady state for clinical efficacy and safety were defined. The PBPK model of OLA can accurately predict the C_{max} and C_{trough} for two formulations in patients administered alone. This has been evidenced by multiple clinical PK study data

| Parameters | Predicted ^a | | | Observed ^a | | |
|----------------------------------------------|------------------------|----------|--------|-----------------------|----------|--------|
| | Mild | Moderate | Severe | Mild | Moderate | Severe |
| Ratio in hepatic impairment patients | | | | | | |
| C_{max} (ng·mL ⁻¹) | 0.99 | 0.87 | 0.94 | 1.14 | 0.74 | NR |
| C_{24} (ng·mL ⁻¹) ^b | 1.1 | 3.1 | 5.7 | 1.29 | 2.02 | |
| AUC_{0-96} (ng·h·mL ⁻¹) | 1.05 | 1.23 | 1.46 | 1.15 | 1.08 | |
| Ratio in renal impairment patients | | | | | | |
| C_{max} (ng·mL ⁻¹) | 1.13 | 1.18 | 1.08 | 1.26 | 1.39 | NR |
| C_{24} (ng·mL ⁻¹) ^b | 1.4 | 3.6 | 6.3 | 1.80 | 2.79 | |
| AUC_{0-96} (ng·h·mL ⁻¹) | 1.19 | 1.57 | 1.76 | 1.62 | 1.75 | |

Table 6. PK parameter (geometric mean) ratios of OLA in patients with hepatic/renal impairment. ^aCalculated by dividing normal data (300 mg OD) with mild, moderate and severe, respectively. ^bPlasma concentration at 24 h.

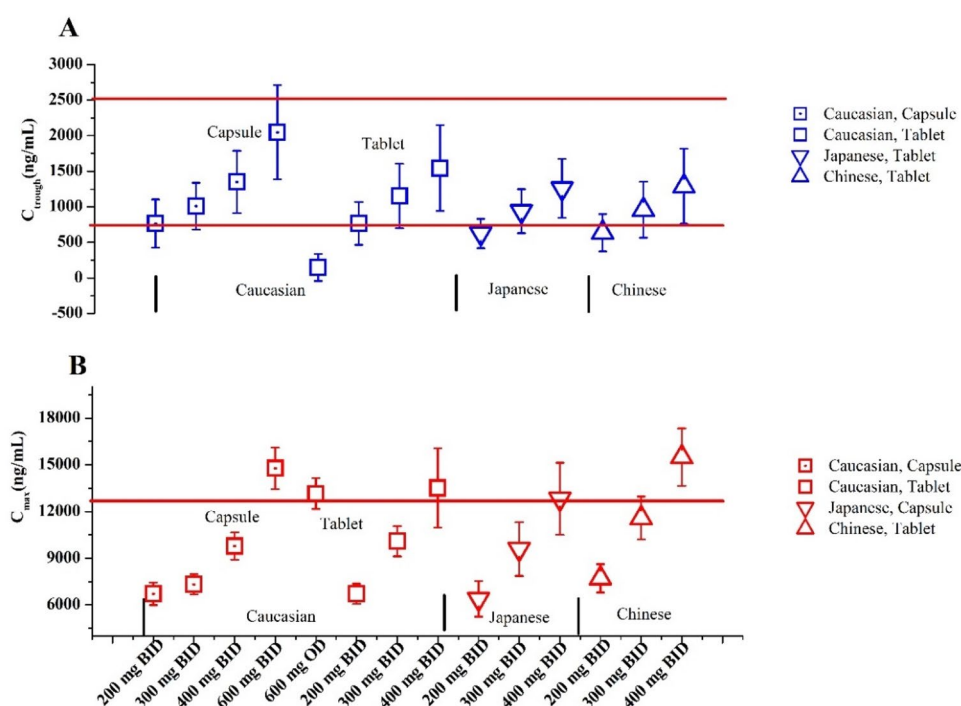


Figure 5. The PBPK simulations of predicted C_{trough} (A) and C_{max} (B) in Caucasian, Japanese and Chinese. Data were shown as geometric mean values and 95%CI. In the simulations, capsule and tablet were administered to Caucasian. Japanese and Chinese only took OLA tablet.

(see Fig. 2 and Table 4). In different inter-ethnic groups, known inter-ethnic physiological differences in height and weight distribution, liver volume, CYP enzyme expression, gastrointestinal transit time, and plasma protein composition have been reported^{17,33}. In this simulation, based on the paper¹⁸, only different liver volume and CYP3A4 abundance data between inter-ethnic populations were incorporated into the PBPK model based on literature data. The default values of the PK-Sim were used for physiological differences in height and weight distribution. The simulations found that, although the geometric mean C_{max} and C_{trough} of OLA in Chinese are lower than those in Caucasian, the predicted C_{max} and C_{trough} values are not statistically significantly different between them (Table 4).

When co-administered with itraconazole and rifampicin, there was good agreement between the PBPK prediction and clinical observation in PK profiles and data (see Table 5 and Fig. 4A,B). It is noteworthy that OLA inhibits its own metabolism through reversible time-dependent inhibition against CYP3A4 as well as enhances its own metabolism through induction of in vivo CYP3A4 expression⁷. The sensitive analysis also demonstrates that the inhibition and induction parameters of OLA had an effect on C_{max} and C_{trough} (see Fig. 3). The PBPK model incorporated CYP3A4 auto-inhibition (K_i) and induction parameters (E_{max} and EC_{50}) to ensure the predictive performance of the model. However, this may not be robust for model. Recent research^{34,35} has also employed the PBPK approach to anticipate clinical DDIs involving combined CYP3A4 inhibitors and inducers, thereby

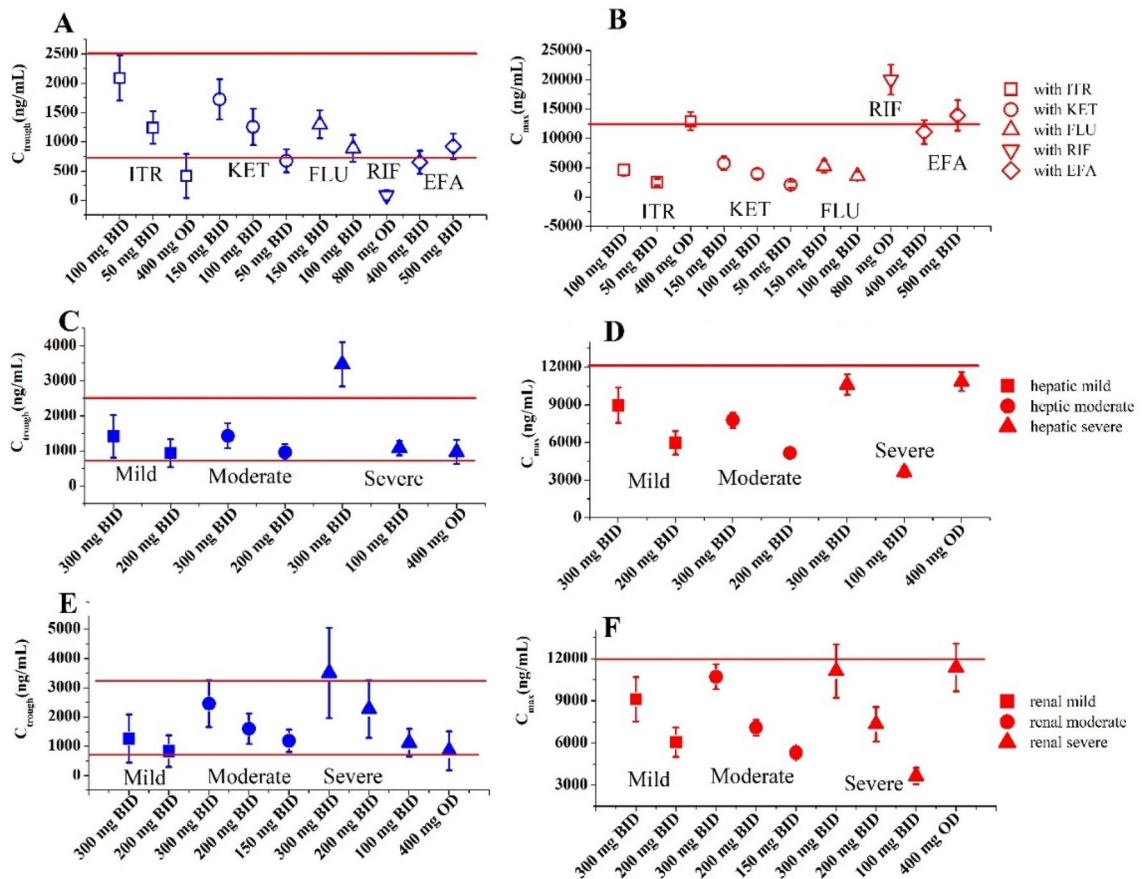


Figure 6. The PBPK simulations of predicted C_{max} and C_{trough} when dosed with other CYP3A4 modulators (A, B), in patients with hepatic impairment (C, D), and with renal impairment (E, F). Data were shown as geometric mean values and 95%CI. ITR: itraconazole, KET: ketoconazole, FLU: fluconazole, RIF: rifampicin, EFA: efavirenz.

providing additional validation for our PBPK approach in assessing the impact of such mixed inhibition and induction. The induction parameter of rifampicin exhibited significant inter-individual variability across various literature studies^{7,36,37}. To mitigate this variability, we incorporated the induction parameter values from the most recent publication⁷ into the current model, where inhibition and induction activity of OLA were also determined concurrently. Use of rifampicin induction parameters may be reasonable based on indirect evidence that our model accurately estimated the induction of intestinal CYP3A4 by rifampicin, with predicted changes showing close agreement with experimentally determined values in humans³⁸ (3.8-fold increase versus 4.4-fold change). The predicted expression of intestinal CYP3A4 after induction by rifampicin was close to the experimentally determined value in humans³⁸ (3.8-fold increase vs. 4.4-fold change).

The PBPK model reasonably predicted hepatic/renal-impairment effects on the PK change of OLA (see Table 6 and Fig. 4C–F). The PBPK model slightly overpredicted PK data in patients with moderate hepatic impairment, especially on C_{24} by 1.5-fold. Prior research has demonstrated that many PBPK models tend to overpredict PK in patients with hepatic impairment²⁸. This is likely because current PBPK models are unable to account for variations in absorption (such as a reduction in bile salt concentration) caused by hepatic impairment. Whereas, given the slight overestimation, fraction absorbed value was not adjusted in this study. Besides, A larger number of studies have described alterations in plasma protein concentration in patients with hepatic/renal impairment^{28,30,39}. Various PPSF values (see Table S2,S3) were utilized in this study to model changes in plasma protein levels among affected patients with different types of impairment.

One published paper has reported the development of a PBPK model for OLA and its dosing considerations in DDIs using classical AUC ratios¹⁶. However, our study differs from this publication in two important aspects. First, we propose PK thresholds for OLA C_{max} (< 12,500 ng/mL) and C_{trough} (772–2500 ng/mL) as key parameters for clinical efficacy and safety. These thresholds, combined with the PBPK model, serve as a crucial strategy for adjusting dosing regimens in DDIs or patients with hepatic/renal impairment. Compared to relying solely on AUC ratios, this combination strategy provides better dosing adjustment, particularly for OLA, which exhibits a nonlinear dose-AUC relationship. Second, we have collected a larger dataset of clinical PK data to develop and validate our PBPK model. This model can predict OLA concentrations not only in Caucasian populations but also in Japanese and Chinese populations. To our knowledge, this is the first investigation to simulate the inter-ethnic PK of OLA across these three different populations.

| Scenarios | C _{max} (ng/mL, 95%CI) | C _{trough} (ng/mL, 95%CI) | AUC ratio | Based-AUC ratio recommendation | Based-model recommendation |
|------------------------------------|---------------------------------|------------------------------------|-----------|----------------------------------|---------------------------------------------------|
| DDI (OLA + Itraconazole 200 mg OD) | | | | | |
| 100 mg BID | 4611 (3970–5874) | 2089 (1785–2754) | 2.85 | Reduce dose to 100 mg BID | Support dose reduction to 50 mg BID |
| 50 mg BID | 2498 (2137–3227) | 1244 (1068–1221) | | | |
| 400 mg OD | 12,903 (11,721–14,850) | 419 (314–1666) | | | |
| DDI (OLA + Ketoconazole 400 mg OD) | | | | | |
| 150 mg BID | 5737 (4939–7253) | 1726 (1401–2693) | 1.73 | Reduce dose to 150 mg BID | Support dose reduction to 100 mg BID |
| 100 mg BID | 3956 (3388–5067) | 1257 (1027–1848) | | | |
| 50 mg BID | 2080 (1768–2711) | 675 (558–952) | | | |
| DDI (OLA + Fluconazole 200 mg OD) | | | | | |
| 150 mg BID | 5234 (4483–6616) | 1299 (1030–1901) | 1.4 | No need to adjust dose | Support dose reduction to 150 mg BID |
| 100 mg BID | 3588 (3063–4552) | 889 (751–1207) | | | |
| DDI (OLA + Rifampicin 600 mg OD) | | | | | |
| 800 mg BID | 20,024 (17,999–23,116) | 86 (30–230) | 0.17 | Avoid concomitant use | Avoid concomitant use |
| DDI (OLA + Efavirenz 600 mg OD) | | | | | |
| 400 mg BID | 11,077 (9704–13,761) | 650 (421–1213) | 0.42 | Increase dose to 600 mg BID | Not recommended |
| 500 mg BID | 13,925 (12,174–17,366) | 923 (598–1432) | | | |
| Hepatic impairment | | | | | |
| Mild | C _{max} (ng/mL, 95%CI) | C _{trough} (ng/mL, 95%CI) | AUC ratio | Based-AUC ratio recommendation | Based-model recommendation |
| 300 mg BID | 8963 (7748–10,560) | 1419 (997–2207) | 1.05 | No need to adjust dose | Supported dose unchanged |
| 200 mg BID | 5968 (5164–7023) | 937 (661–1450) | | | |
| Moderate | | | | | |
| 300 mg BID | 7782 (7199–8457) | 1430 (1148–1854) | 1.23 | No need to adjust dose | Support dose reduction to 200 mg BID |
| 200 mg BID | 5161(4786–5616) | 967 (752–1215) | | | |
| Severe | | | | | |
| 300 mg BID | 10,616 (9853–11,495) | 3468 (2938–4191) | 1.46 | No need to adjust dose | Support dose reduction to 100 mg BID or 400 mg OD |
| 100 mg BID | 3639 (3259–4109) | 1081 (914–1323) | | | |
| 400 mg OD | 10,853 (10,145–11,654) | 976 (726–1413) | | | |
| Renal impairment | | | | | |
| Mild | | | | | |
| 300 mg BID | 9108 (7700–10,886) | 1263 (715–2359) | 1.19 | No need to adjust dose | Supported dose unchanged |
| 200 mg BID | 6063 (5133–7237) | 834 (475–1553) | | | |
| Moderate | | | | | |
| 300 mg BID | 10,707 (9889–11,649) | 2456 (1864–3459) | 1.57 | Reduce dose to 200 mg BID | Support dose reduction to 150 mg BID |
| 200 mg BID | 7095 (6564–7706) | 1601 (1217–2248) | | | |
| 150 mg BID | 5313 (4919–5765) | 1192 (607–1670) | | | |
| Severe | | | | | |
| 300 mg BID | 11,114 (9493–13,288) | 3506 (2477–5556) | 1.76 | Reduce dose to 200 or 150 mg BID | Support dose reduction to 100 mg BID |
| 200 mg BID | 7334 (6287–8731) | 2274 (1616–3584) | | | |
| 100 mg BID | 3652 (3144–4326) | 1120 (802–1751) | | | |
| 400 mg OD | 11,374 (9914–13,290) | 847 (534–1857) | | | |

Table 7. OLA dosing adjustment recommendations based on the PBPK model.

For most therapeutic drug, if the exposure ratio increases or reduces by more than twofold, it may be necessary to consider clinical dosage adjustments (widely acceptable clinically significant criteria⁴⁰). However, the systemic exposure (AUC) of OLA does not increase in direct proportion to dose within the 100–400 mg dose range⁴. The adjustment of the dosage regimen for OLA cannot be straightforward on the basis of an AUC change. The exposure–response relationship for both efficacy and safety has defined the PK thresholds of OLA C_{max} (< 12,500 ng/mL) and C_{trough} (772–2500 ng/mL). This study proposes that using PK thresholds for OLA may be a superior approach to dosing adjustment in multiple clinical scenarios based on PK thresholds of OLA C_{max} and C_{trough}.

The optimal dosing regimens of OLA for each of the ethnic populations were first studied based on the geometric mean and 95%CI of predicted C_{max} and C_{trough}. This strategy for optimal dosing has been proposed by Johnson et al.⁴¹ and Adiwidjaja et al.¹⁸. Based on this strategy, it was suggested that a dosing regimen consisting of 300 or 400 mg BID in capsule formulation, as well as 300 mg BID in tablet formulation, may be considered an optimal option for three different inter-ethnic patient populations (see Fig. 5). When dosed in combination with CYP3A4 inhibitors (strong and moderate), our PBPK model indicated that dosing regimens for OLA may

be modified to either 50 mg BID or 150 mg BID (see Table 7 and Fig. 6A,B). Given the available approved tablets with strengths of 100 and 150 mg, our analysis suggests that dosing regimens for OLA should be adjusted to 100 mg BID when administered along with a potent CYP3A4 inhibitor and to 150 mg BID with a moderate CYP3A4 inhibitor. The recommendation is in good agreement with the clinical recommendations². Conversely, when dosed in combination with CYP3A4 inducers (strong and moderate), it is not suggested to co-administer with CYP3A4 inducers based on the PBPK model (see Table 7 and Fig. 6A,B). The recommendation is also in good agreement with the clinical recommendations². However, except for co-administration with rifampicin, dosing adjustment recommendations of OLA in DDIs by the PBPK model are different from the recommendations by the AUC ratios, particularly in co-administration with efavirenz. The dosing adjustment recommendations are the same for patients with mild hepatic/renal impairment between the PBPK model and AUC ratio. The dosage adjustment by the PBPK model suggested 200 mg BID and 100 mg BID (or 400 mg OD) represent an appropriate dosing schedule for patients with moderate or severe hepatic impairment, respectively. This is completely different from the recommendations based on the AUC ratio (see Table 7). This is most likely due to a more sensitive change in C_{max} and C_{trough} than in AUC. The dosage adjustment by the PBPK model suggested 150 mg BID and 100 mg BID represent a suitable dosing regimen for patients with moderate and severe renal impairment, respectively, which is lower dosing than the recommendations by AUC ratio (see Table 7). The recommendation of a dose reduction to 150 mg BID for patients with moderate renal impairment is slightly different from the clinical study (dosage reduction to 200 mg BID)². The simulations in the Japanese and Chinese populations could not be validated using the available clinically observed PK data for DDIs and patients with hepatic/renal impairment, which were solely obtained from the Caucasian population. Moreover, significant differences were not found in the predicted in predicted C_{max} and C_{trough} values at steady state (Fig. 5). Therefore, the simulations for DDIs and patients with hepatic/renal impairment were exclusively conducted using the Caucasian population in this study.

However, there are certain limitations to the current model. First, the dosing adjustment for hepatically impaired patients has not been verified using any clinical study data. Another challenge associated with this PBPK approach is the absence of consideration in the PBPK model role of other inter-ethnic physiological differences, except for differences in height and weight distribution, liver volume, and CYP enzyme expression.

Conclusion

In conclusion, the PBPK models adequately predicted the clinical PK data of OLA in three inter-ethnic populations, adequately provided DDI prediction with CYP3A4 modulators, and accurately simulated PK change in patients with hepatic/renal impairment. Finally, a dosage adjustment strategy was proposed to modify the OLA dosing regimens using this PBPK model in multiple clinical scenarios.

Data availability

All the data generated during the research is either reported in the manuscript or is provided in the supplementary file.

Received: 3 June 2023; Accepted: 21 September 2023

Published online: 25 September 2023

References

- Deeks, E. D. Olaparib: First global approval drugs February. *Drugs*. **75**, 231–240 (2015).
- National library of medicine. Accessed 1 Jun 2023. <https://dailymed.nlm.nih.gov/dailymed/drugInfo.cfm?setid=741ff3e3-dc1a-45a6-84e5-2481b27131aa>.
- Dirix, L. *et al.* Effect of itraconazole and rifampin on the pharmacokinetics of olaparib in patients with advanced solid tumors: results of two phase I open-label studies. *Clin Ther.* **38**, 2286–2299 (2016).
- Food and Drug Administration (FDA). Accessed 1 Jun 2023. https://www.accessdata.fda.gov/drugsatfda_docs/nda/2017/208558Orig1s000MultidisciplineR.pdf.pdf.
- Song, Y. K. *et al.* Role of the efflux transporters Abcb1 and Abcg2 in the brain distribution of olaparib in mice. *Eur J Pharm Sci* **173**, 106177 (2022).
- McCormick, A. & Swaisland, H. J. X. In vitro assessment of the roles of drug transporters in the disposition and drug–drug interaction potential of olaparib. *Xenobiotica* **47**, 903–915 (2017).
- McCormick, A., Swaisland, H., Reddy, V. P., Learoyd, M. & Scarfe, G. J. X. In vitro evaluation of the inhibition and induction potential of olaparib, a potent poly (ADP-ribose) polymerase inhibitor, on cytochrome P450. *Xenobiotica* **48**, 555–564 (2018).
- Meneer, K. A. *et al.* 4-[3-(4-cyclopropanecarbonylpiperazine-1-carbonyl)-4-fluorobenzyl]-2 H-phthalazin-1-one: a novel bioavailable inhibitor of poly (ADP-ribose) polymerase-1. *J. Med. Chem.* **51**, 6581–6591 (2008).
- Kaye, S. B. *et al.* Phase II, open-label, randomized, multicenter study comparing the efficacy and safety of olaparib, a poly (ADP-ribose) polymerase inhibitor, and pegylated liposomal doxorubicin in patients with BRCA1 or BRCA2 mutations and recurrent ovarian cancer. *J. Clin. Oncol.* **30**, 372–379 (2012).
- Fong, P. C. *et al.* Inhibition of poly (ADP-ribose) polymerase in tumors from BRCA mutation carriers. *N Engl. J. Med.* **361**, 123–134 (2009).
- Dean, E. *et al.* Phase I study to assess the safety and tolerability of olaparib in combination with bevacizumab in patients with advanced solid tumours. *Br. J. Cancer.* **106**, 468–474 (2012).
- Yamamoto, N. *et al.* A Phase I, dose-finding and pharmacokinetic study of olaparib (AZD2281) in Japanese patients with advanced solid tumors. *Cancer Sci.* **103**, 504–509 (2012).
- Velev, M. *et al.* Association between olaparib exposure and early toxicity in BRCA-mutated ovarian cancer patients: results from a retrospective multicenter study. *Pharmaceuticals* **14**, 804 (2021).
- Rolfo, C. *et al.* Pharmacokinetics and safety of olaparib in patients with advanced solid tumours and renal impairment. *Clin. Pharmacokinet.* **58**, 1165–1174 (2019).
- Basit, A. *et al.* Kidney cortical transporter expression across species using quantitative proteomics. *Drug. Metab. Dispos.* **47**, 802–808 (2019).

16. Pilla Reddy, V. *et al.* Physiologically based pharmacokinetic modeling for olaparib dosing recommendations: bridging formulations, drug interactions, and patient populations. *Clin. Pharmacol. Ther.* **105**, 229–241 (2019).
17. Matsumoto, Y. *et al.* Application of physiologically based pharmacokinetic modeling to predict pharmacokinetics in healthy Japanese subjects. *Clin. Pharmacol. Ther.* **105**, 1018–1030 (2019).
18. Adiwidjaja, J., Gross, A. S., Boddy, A. V. & McLachlan, A. J. Physiologically-based pharmacokinetic model predictions of inter-ethnic differences in imatinib pharmacokinetics and dosing regimens. *Br. J. Clin. Pharmacol.* **88**, 1735–1750 (2022).
19. Pharmaceuticals and Medical Devices Agency (PMDA). Accessed 1 Jun 2023. https://www.info.pmda.go.jp/go/interview/1/670227_4291052F1027_1_111_1E.pdf.
20. Yonemori, K. *et al.* Safety and tolerability of the olaparib tablet formulation in Japanese patients with advanced solid tumours. *Cancer Chemother. Pharmacol.* **78**, 525–531 (2016).
21. Yuan, P. *et al.* Pharmacokinetics and safety of olaparib tablets as monotherapy and in combination with paclitaxel: Results of a Phase I study in Chinese patients with advanced solid tumours. *Cancer Chemother. Pharmacol.* **83**, 963–974 (2019).
22. Mateo, J. *et al.* An adaptive study to determine the optimal dose of the tablet formulation of the PARP inhibitor olaparib. *Target. Oncol.* **11**, 401–415 (2016).
23. Plummer, R. *et al.* Pharmacokinetic effects and safety of olaparib administered with endocrine therapy: A phase I study in patients with advanced solid tumours. *Adv. Ther.* **35**, 1945–1964 (2018).
24. Saeheng, T., Na-Bangchang, K., Siccardi, M., Rajoli, R. K. R. & Karbwang, J. Physiologically-based pharmacokinetic modeling for optimal dosage prediction of quinine coadministered with ritonavir-boosted lopinavir. *Clin. Pharmacol. Ther.* **107**, 1209–1220. <https://doi.org/10.1002/cpt.1721> (2020).
25. Food and Drug Administration (FDA). Accessed 1 Jun 2023. https://www.accessdata.fda.gov/drugsatfda_docs/nda/2017/210259Orig1s000MultidisciplineR.pdf.
26. Li, G. *et al.* Effect of CYP3A4 inhibitors and inducers on pharmacokinetics and pharmacodynamics of saxagliptin and active metabolite M2 in humans using physiological-based pharmacokinetic combined DPP-4 occupancy. *Front. Pharmacol.* **12**, 746594 (2021).
27. Salerno, S. N. *et al.* Physiologically-based pharmacokinetic modeling characterizes the CYP3A-mediated drug-drug interaction between fluconazole and sildenafil in infants. *Clin. Pharmacol. Ther.* **109**, 253–262 (2021).
28. Heimbach, T. *et al.* Physiologically-based pharmacokinetic modeling in renal and hepatic impairment populations: a pharmaceutical industry perspective. *Clin. Pharmacol. Ther.* **110**, 297–310 (2021).
29. Willmann, S. *et al.* Applications of physiologically based pharmacokinetic modeling of rivaroxaban—Renal and hepatic impairment and drug-drug interaction potential. *J. Clin. Pharmacol.* **61**, 656–665 (2021).
30. Rolfo, C. *et al.* Pharmacokinetics and safety of olaparib in patients with advanced solid tumours and mild or moderate hepatic impairment. *Br. J. Clin. Pharmacol.* **86**, 1807–1818 (2020).
31. Wu, C. *et al.* Prediction for optimal dosage of pazopanib under various clinical situations using physiologically based pharmacokinetic modeling. *Front. Pharmacol.* **13**, 963311 (2022).
32. Malik, P. R. *et al.* A physiological approach to pharmacokinetics in chronic kidney disease. *J. Clin. Pharmacol.* **60**, S52–S62 (2020).
33. Barter, Z. E., Tucker, G. T. & Rowland-Yeo, K. Differences in cytochrome p450-mediated pharmacokinetics between chinese and caucasian populations predicted by mechanistic physiologically based pharmacokinetic modelling. *Clin. Pharmacokinet.* **52**, 1085–1100 (2013).
34. Yu, Y., Loi, C. M., Hoffman, J. & Wang, D. Physiologically based pharmacokinetic modeling of palbociclib. *J. Clin. Pharmacol.* **57**, 173–184 (2017).
35. Yamazaki, S., Johnson, T. R. & Smith, B. J. Prediction of drug-drug interactions with crizotinib as the CYP3A substrate using a physiologically based pharmacokinetic model. *Drug Metab. Dispos.* **43**, 1417–142 (2015).
36. Hanke, N. *et al.* PBPK models for CYP3A4 and P-gp DDI prediction: a modeling network of rifampicin, itraconazole, clarithromycin, midazolam, alfentanil, and digoxin. *CPT Pharmacomet. Syst. Pharmacol.* **7**, 647–659 (2018).
37. Asaumi, R. *et al.* Comprehensive PBPK model of rifampicin for quantitative prediction of complex drug-drug interactions: CYP3A/2C9 induction and OATP inhibition effects. *CPT Pharmacomet. Syst. Pharmacol.* **7**, 186–196 (2018).
38. Greiner, B. *et al.* The role of intestinal P-glycoprotein in the interaction of digoxin and rifampin. *J. Clin. Invest.* **104**, 147–153 (1999).
39. O'Bryant, C. L. *et al.* An open-label study to describe pharmacokinetic parameters of erlotinib in patients with advanced solid tumors with adequate and moderately impaired hepatic function. *Cancer Chemother. Pharmacol.* **69**, 605–612 (2012).
40. Wagner, C., Pan, Y., Hsu, V., Sinha, V. & Zhao, P. Predicting the effect of CYP3A inducers on the pharmacokinetics of substrate drugs using physiologically based pharmacokinetic (PBPK) modeling: an analysis of PBPK submissions to the US FDA. *Clin. Pharmacokinet.* **55**, 475–483 (2016).
41. Johnson, T. N. *et al.* Development of a physiologically based pharmacokinetic model for mefloquine and its application alongside a clinical effectiveness model to select an optimal dose for prevention of malaria in young Caucasian children. *Br. J. Clin. Pharmacol.* **85**, 100–113 (2019).

Acknowledgements

Thanks are due to Guopeng Wang and Honghai Wu for assistance and cooperation.

Author contributions

D.G. wrote the manuscript text and prepared all tables and figures; H.W. was responsible for data curation. G.W. was responsible for software calculation. J.R. contributed to investigation, methodology conceptualization, formal analysis, and supervision. All authors reviewed the manuscript.

Funding

This research did not receive any specific grant from funding agencies in the public, commercial, or not-for-profit sectors.

Competing interests

Author Guopeng Wang is employed by Zhongcai Health (Beijing) Biological Technology Development Co., Ltd.. The remaining authors declare that the research was conducted in the absence of any commercial or financial relationships that could be construed as a potential conflict of interest.

Additional information

Supplementary Information The online version contains supplementary material available at <https://doi.org/10.1038/s41598-023-43258-9>.

Correspondence and requests for materials should be addressed to J.R.

Reprints and permissions information is available at www.nature.com/reprints.

Publisher's note Springer Nature remains neutral with regard to jurisdictional claims in published maps and institutional affiliations.



Open Access This article is licensed under a Creative Commons Attribution 4.0 International License, which permits use, sharing, adaptation, distribution and reproduction in any medium or format, as long as you give appropriate credit to the original author(s) and the source, provide a link to the Creative Commons licence, and indicate if changes were made. The images or other third party material in this article are included in the article's Creative Commons licence, unless indicated otherwise in a credit line to the material. If material is not included in the article's Creative Commons licence and your intended use is not permitted by statutory regulation or exceeds the permitted use, you will need to obtain permission directly from the copyright holder. To view a copy of this licence, visit <http://creativecommons.org/licenses/by/4.0/>.

© The Author(s) 2023